A Robust Strategy for Leveraging Soft Open Points to Mitigate Load Altering Attacks

Zhaoxi Liu, *Member, IEEE,* and Lingfeng Wang, *Senior Member, IEEE*

***Abstract*—Power system cybersecurity is emerging as a critical and urgent problem to the energy sector due to the ongoing power grid modernization initiative. Load altering attack (LAA) is an important category of cyberattacks on the modern power systems, in which the attackers may damage the grid by viciously altering the remotely controllable loads (RCL) that are not properly protected. In order to mitigate the impacts of LAAs on the distribution systems, the promising soft open point (SOP) technology is deployed in this study. A two-stage optimization framework is proposed for the optimal installation and operation of SOPs for defending the distribution systems against LAAs. A chance-constrained optimization model is developed to guarantee the confidence level of the proposed two-stage model of SOPs in mitigating the impacts of LAAs. Further, a Wasserstein metric based distributionally robust chance-constrained (DRCC) optimization method is developed to ensure the robustness of the proposed model against the ambiguity of the empirical probability distribution in practice. Case studies were performed on a 69-bus test system to validate the proposed method. The results of case studies show that the proposed framework is able to mitigate the impacts of LAAs on distribution systems with the installation of SOPs. By applying the DRCC optimization method, the proposed model manages to keep satisfactory confidence levels under the ambiguous probability distributions in the case studies.**

***Index Terms*—Active distribution network, cybersecurity, distributionally robust chance-constrained optimization, load altering attack, soft open point.**

NOMENCLATURE

A. Indices and Sets:

a	Index of load altering attack (LAA) actions.
i, j	Index of buses in distribution system (DS).
i'	Index of parent node of bus i.
i''	Index of children nodes of bus i.
ω, ω'	Index of scenarios.
ψ	Index of soft open points (SOPs).
$\mathcal{A}$	Set of LAA actions.
$\mathcal{D}$	Ambiguity set of probability distribution.
$\mathcal{N}$	Set of buses.
$\mathcal{N}_i$	Set of children nodes of bus i.
$\mathcal{N}_\psi$	Set of buses connected to SOP ψ.
Ω	Set of scenarios.
Ψ	Set of installed SOPs.
$\widetilde{\Psi}$	Set of SOP installation candidates.

This work was supported by the U.S. National Science Foundation Industry/University Cooperative Research Center on Grid-connected Advanced Power Electronic Systems (GRAPES) under Award GR-18-06.

Zhaoxi Liu and Lingfeng Wang are with Department of Electrical Engineering and Computer Science, University of Wisconsin-Milwaukee, Milwaukee, WI 53211 USA (e-mail: zhaoxil@uwm.edu, l.f.wang@ieee.org).

B. Parameters:

A_i	Loss coefficient of SOP.
P_i^L	Active power of loads at bus i in DS.
P_i^A	Active power of loads altered by LAAs at bus i.
Q_i^L	Reactive power of loads at bus i in DS.
Q_i^A	Reactive power of loads altered by LAAs at bus i.
M	A large enough positive constant.
r_i	Resistance of branches in DS.
x_i	Reactance of branches in DS.
S_i^{max}	Capacity limit of branches in DS.
V^{max}	Upper limit of bus voltage.
V^{min}	Lower limit of bus voltage.
α, β	Cost coefficients of SOP installation.
ξ_i^{max}	Upper reactive power limit coefficient of SOP.
ξ_i^{min}	Lower reactive power limit coefficient of SOP.
ρ	Wasserstein distance limit of ambiguity set.
ε	Probability coefficient of chance constraint for scenario ω.
ϖ_ω	Empirical probability of scenario ω.

C. Variables:

P_i	Active power flow of branches in DS.
P_i^{SOP}	Active power of SOP at bus i.
$P_i^{SOP,L}$	Power loss of SOP converter connected to bus i.
Q_i	Reactive power flow of branches in DS.
Q_i^{SOP}	Reactive power of SOP at bus i.
S_i	Capacity of SOP converter connected to bus i.
V_i	Voltage of buses in DS.
I_i, U_i	Intermediate variables for second-order cone programming (SOCP) formulation of DistFlow.
u_ω	Intermediate variable of chance constraint.
z_ψ	Installation decision of SOP.
π_ω	Probability of scenario ω.
$\lambda_{\omega,\omega'}$	Probability with joint distribution in ambiguity set $\mathcal{D}$.
$\delta_{\omega'}, \zeta_\omega$	Dual variables of equality constraints of the optimization for calculating Wasserstein distance.
$\mu_{\omega,\omega'}$	Dual variables of lower limit constraints of $\lambda_{\omega,\omega'}$ in the optimization for calculating Wasserstein distance.
$\nu_{\omega,\omega'}$	Dual variables of upper limit constraints of $\lambda_{\omega,\omega'}$ in the optimization for calculating Wasserstein distance.

D. Functions:

$\mathcal{F}_{SOP}$ Objective function of optimization model for SOP installation and sizing decisions.

I. Introduction

In recent years, a massive transformation is ongoing in the power systems towards a more flexible, efficient and smarter electric grid with the fast-developing operational technology (OT) and information technology (IT) in the power systems. Consequently, cyber vulnerability of the grid is introduced across all levels of power systems [1], [2]. As the consequences of an effective cyberattack against the power systems can be extreme and disturbing the normal operation of the grid can have tremendous financial and security effects to the entire society, the power systems have become a primary target of the cyberattacks by malicious adversaries. A real-world example is the two effective cyberattacks against the Ukrainian power system in 2015 and 2016 [3]. By the first attack in 2015, about 225 thousand residents in three provinces of Ukraine were affected for up to 6 hours [4]. Over 130 MW of loads were lost and more than 50 substations were disconnected from the grid viciously by the attackers. Therefore, the cybersecurity of power systems against malicious cyberattacks is emerging as a critical and urgent topic for the entire society.

Load altering attack (LAA) is an important category of cyberattacks on the modern power systems. The attacker of LAAs attempts to maliciously alter a group of remotely controllable loads (RCL) that are not properly secured to damage the grid through circuit overloads and/or other mechanisms [5], [6]. Research [5] identifies the practical loads that are vulnerable to the Internet-based LAAs and overviews the defense mechanisms to block the attacks and limit the damage. Reference [6] studies the dynamic LAAs against the frequency stability of the power system. In the research, the fundamental characteristics of the attack models are analyzed and explained. Meanwhile, the protection schemes against the dynamic LAAs are designed and proposed in the study. In [7], the risks of system-wide unstable oscillations and trips of generators in the grid due to LAAs are investigated. The vulnerability of the smart grid under LAAs is analyzed in [8] using a graph theory based method. An anomaly detection scheme of power consumption is proposed in [9] to indicate potential malicious LAAs on the grid. The existing researches on LAAs mentioned above mainly focus on the damage and influence of LAAs on the generation and transmission sides of the grid. The impacts of LAAs on the distribution systems have not been covered in the existing literature. However, LAAs may cause more direct and damaging results on the distribution systems. Thus, in this paper, the impacts of LAAs on the distribution systems are studied.

In order to enhance the robustness of the distribution systems against malicious attacks, the system operation should be reinforced. Recently, soft open points (SOPs) are emerging as a promising power electronics based interconnection solution in the distribution networks to enhance the controllability and flexibility of the system operation. A series of recent researches have explored the application of SOPs to improve the flexibility of distribution systems. In [10], the benefits of employing SOPs and other power electronic devices to support growing distributed generation (DG) are analyzed. The operation principle of SOPs in distribution systems is proposed in [11], and an optimal operation model of SOPs in distribution networks is proposed in [12]. In [13], the dynamic performance of a medium voltage (MV) distribution network with a connected SOP under grid side AC faults is investigated. The bi-level optimization model proposed in [14] considers the planning of converter-based DG units and SOPs in a coordinated way for incorporating active management of the unbalanced distribution networks. The three-Phase unbalanced conditions of the distribution networks are also considered in the optimal operation model of SOPs in [15]. In [16], a three-terminal MV SOP topology is proposed for the distribution systems with renewable energy sources (RES), and the DC voltage control strategy of the three-terminal SOP is studied. The control method of a back-to-back SOP in the distribution systems to mitigate the voltage fluctuation caused by DG is studied in [17]. A coordinated control method of voltage and reactive power of the distribution systems based on SOPs is proposed in [18] to manage the increasing penetration of DG in distribution networks. In [19], a voltage regulation framework is proposed for distribution systems through the SOPs and the DG inverters. A two-stage robust optimization model is built for the operation of SOPs in [20] to handle the uncertainties of photovoltaic (PV) generation in the distribution systems.

The existing literature has provided valuable insights on the potential of SOPs in improving the distribution system operation. However, the implementation and operation strategies of SOPs in the grids against malicious cyberattacks on the distribution networks have not been studied in the existing researches. In this paper, the back-to-back SOP is employed to mitigate the impacts of malicious LAAs on the distribution systems. A chance-constrained model which considers the operation of the SOPs against LAAs is developed to determine the optimal installation and sizing decisions of SOPs in a set of installation candidates. In the existing literature, most of the studies focus on the optimal operation and control strategies of the SOPs in different scenarios, e.g., [11]–[13], [15]–[20]. In these works, the deployment strategy of SOPs is not considered. However, the operation constraints of the SOPs in these works are consistent with the constraints in the proposed models in this paper. The models in these works are compatible with the proposed SOP installation and sizing model and SOP operation strategy against LAAs. In other scenarios (e.g., normal scenarios, AC faults, etc.), the distribution system operator (DSO) may operate the SOPs with the existing models in literature according to his/her interest and perspective in the corresponding scenario. When successful LAAs are launched on the distribution system, the DSO may apply the proposed operation strategy of the SOPs in this paper to mitigate the impacts of the attacks. In [14], a coordinated DG-SOP planning model is proposed to minimize the investment and operation costs. In this paper, only the investment cost of the SOP installation is considered. However, it is feasible to extend the proposed model in this paper to consider the total cost of the SOP installation and

operation with proper modification on the optimization model. Nevertheless, due to the chance constraints on the security of the distribution network under potential attacks, the proposed model is subject to additional limits, and the expected total cost of the SOP installation and operation is supposed to be higher than the case not considering the security constraints. The higher cost is paid to enhance the robustness and resilience of the distribution network against malicious attacks.

In the generic chance-constrained programming framework, the probability distribution of scenarios is needed and applied in the chance constraint. In practical applications, the estimated distribution is usually used to solve the optimization model. However, the actual probability distribution may deviate from the estimated distribution in practice. As a result, the required confidence level in the chance constraint of the model is no longer guaranteed. To this end, a distributionally robust chance-constrained (DRCC) model is proposed in this paper to improve the robustness of the chance-constrained model against the probability distribution deviation. The Wasserstein metric based distributionally robust optimization technique is applied in the proposed chance-constrained model to provide robustness of the solution against ambiguity. The Wasserstein distance based distributionally robust optimization models have been proposed and studied for the power system operation problems in a few recent researches. For example, a DRCC dispatch model is developed in [21] with Wasserstein distance considering the renewable forecasting errors. In [22], a Wasserstein metric based distributionally robust approximate framework (WDRA) is proposed for the unit commitment problem with wind power forecasting errors. A few generic analyses on the Wasserstein metric based distributionally robust optimization modeling have also been performed recently. In [23], a reformulation of the Wasserstein ball with finite convex optimization problems is proposed. However, to the best knowledge of the authors, the optimal SOP installation and operation problem against LAAs considered in this paper has not been covered or studied in the existing literature. The objective of the proposed work is to provide a robust and flexible solution for the optimal SOP installation and operation decisions against potential LAAs on the distribution networks. While considering the detailed operation strategies of the SOPs in the LAAs, the proposed DRCC model determines the installation decisions of the SOPs in the candidate set of sites and optimizes the sizing of the SOPs to be installed to mitigate the impacts of potential LAAs. Thus, the proposed two-stage model considers both the optimal installation and operation decisions of the SOPs in the distribution networks.

The contributions of this paper are summarized as follows:

- A two-stage optimization framework is proposed to mitigate the impacts of LAAs on the distribution systems with the installation of SOPs. The proposed framework manages the optimal planning and operation of the SOPs for defending the distribution systems against the LAAs.
- A chance-constrained optimization model is developed to achieve the confidence level of the proposed installation and operation models of SOPs in thwarting the LAAs on the distribution systems. The Wasserstein distance based distributionally robust optimization technique is applied in the chance-constrained SOP installation and sizing problem to robustize the SOP installation strategy against potential LAAs. A corresponding master and sub-problem based algorithm is developed to solve the proposed DRCC model.

The rest of the paper is organized as follows. Section II gives a concise introduction of the LAAs on the distribution systems. In Section III, the optimal installation and operation models of SOPs to mitigate the impacts of LAAs are described in detail. Then, the Wasserstein metric based DRCC model is proposed in Section IV. In Section V, the case studies of the proposed model are presented, followed by the conclusions in Section VI.

II. Load Altering Attacks on Distribution Networks

In the LAAs, the attackers attempt to damage the power system by maliciously altering a set of controllable loads that are not properly secured. In practice, a wide range of loads can be vulnerable to LAAs, including remotely controllable loads, loads that automatically respond to price or are controlled by direct load control (DLC) command signals, and frequency-responsive loads [5], [6]. In the distribution networks, the volumes of such controllable and responsive loads (e.g., electric vehicles (EVs) and smart appliances) are increasing in recent years with the trend towards the smart grid and active distribution systems. However, due to the high cost of expanding/upgrading the distribution systems, advanced resource optimization techniques are used to accommodate the increasing loads and allow some inherent physical redundancy within the systems to be reduced in the operation [24]–[26], which also decrease the resilience of the distribution systems against successful cyberattacks. Thus, the impacts of LAAs can be damaging to the normal operation of distribution systems.

The LAA is a realistic attack scenario on power systems. Due to the rapidly increasing amount of flexible demand with automatic and remote control in the smart grid, the vulnerabilities to LAAs are introduced with the widely applied information systems to facilitate more advanced functions to better supply the demand. The research in [5] has studied and identified a series of practical loads in the consumption sector of power systems that can be vulnerable to LAAs. Reference [27] reports and analyzes the real-world cybersecurity flaws and vulnerabilities in the smart EV charging systems which may suffer from LAAs. Real-world cybersecurity vulnerabilities and incidents of the heating, ventilation and air conditioning (HVAC) control systems and building management systems (BMS) have also been reported [28].

The adversaries may aim to interrupt the normal operation of the grid by LAAs. Unlike other cyberattacks on the power systems (e.g., switching attacks, false data injection (FDI) attacks), the LAAs do not need to break through the information or control systems of the system operator, which are usually well isolated and protected. It makes LAAs much easier and more realistic for the attackers to prepare and perform the attacks. Meanwhile, another motivation of the adversaries to

launch LAAs can be to disturb the optimal energy management and demand response programs of the flexible loads. Usually, the smart devices of such demand are shifted from the peak hours to the valley hours for lower electricity bills with time-of-use (TOU) or other dynamic pricing schemes, which help reduce the stress of the grid. However, in the LAAs, the adversaries may interfere the optimal energy management by turning on the flexible loads at the peak hours when the electricity prices are the highest. Consequently, the normal operation of the grid can be interrupted due to the impacts of LAAs.

In a successful LAA attempt, the attacker can turn on the RCL that are compromised by the attack at the victim bus simultaneously. The redundancy of the distribution network may not be able to cover such a pulse of the demand. As a result, the distribution system may face overload problems in the branches and/or low voltage problems at the buses, and the network constraints of the distribution system may not be able to be satisfied. Thus, it is important to search for effective measures to mitigate the impacts of successful LAAs on the distribution systems.

In this study, the proposed SOP installation and operation models aim to mitigate the impacts of potential LAAs on the distribution networks. The objective and benefits of the proposed strategies are avoiding network constraint violations, unwanted load curtailment and tripping of the feeders when successful LAAs are launched on the distribution systems. With the proposed chance-constrained SOP installation model and operation strategy, the probability of network constraint violations (and consequent load curtailment and/or tripping of feeders) in the distribution network is limited below a predefined acceptable confidence level under potential LAAs.

III. Optimal Installation and Operation Strategies of SOPs Against LAAs

In order to mitigate the impacts of the LAAs on the distribution systems, an optimal SOP installation and operation model is developed in this paper. The detailed formulation of the proposed model is presented in this section.

A. Power Flow Formulation

In this study, the DistFlow model [29] is applied to formulate the power flow of the distribution system. The DistFlow formulation can accurately model the power flow in radial AC distribution networks [29], [30]. Thus, it is widely used in the distribution system power flow modeling. Existing studies on the optimal planning and operation problems of distribution systems have shown that the DistFlow model can achieve high accuracy in the solutions [31]–[33]. The formulation of the DistFlow model is presented as follows.

$$\sum_{i'' \in \mathcal{N}_i} P_{i''} = P_i - r_i \frac{P_i^2 + Q_i^2}{V_{i'}^2} - P_i^L \tag{1}$$

$$\sum_{i'' \in \mathcal{N}_i} Q_{i''} = Q_i - x_i \frac{P_i^2 + Q_i^2}{V_{i'}^2} - Q_i^L \tag{2}$$

$$V_i^2 = V_{i'}^2 - 2\left(r_i P_i + x_i Q_i\right) + \left(r_i^2 + x_i^2\right) \frac{P_i^2 + Q_i^2}{V_{i'}^2} \tag{3}$$

where i' denotes the parent node of bus i, $\mathcal{N}_i$ is the set of children nodes of bus i, P_i and Q_i denote the active and reactive power flows from the parent node i' to the branch connected to bus i, and V_i is the voltage of bus i in the network. The branch flow model of the DistFlow formulation is demonstrated in Fig. 1. The generic DistFlow model is non-convex which makes it difficult to solve in optimization models. Thus, in this study, a second-order cone reformulation of the DistFlow model is applied. The detailed formulation will be presented in Section III-C. The linearized DistFlow model which neglects the loss terms in the power flow has also been widely applied in literature [34], [35]. However, the DistFlow model is not linearized in the proposed model in this paper and the losses in the distribution network are considered.

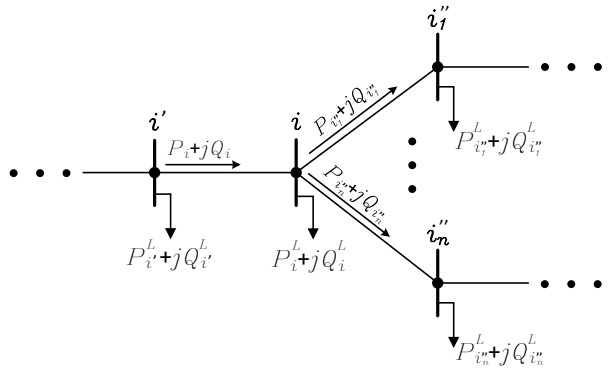

Fig. 1. DistFlow Model for Radial Distribution Networks.

B. SOP Operation Modeling

In this paper, the SOPs are applied in the distribution network to enhance the flexibility of the system operation. An SOP can be installed between two feeders in the distribution system to precisely regulate the power flow. The back-to-back voltage source converters (VSCs) are well accepted for the power system applications as they can accurately adjust the power flow while providing voltage support and reactive power compensation to the grid [15], [18]. Thus, in this study, the back-to-back VSCs are applied for the SOP application in the distribution system. The operation of the SOPs needs to regulate both the active and reactive power outputs of the two converters in the back-to-back VSCs. The constraints for the operation of the back-to-back VSC-based SOPs can be formulated as follows [14], [15].

$$P_i^{SOP} + P_i^{SOP,L} + P_j^{SOP} + P_j^{SOP,L} = 0 \tag{4}$$

$$P_i^{SOP,L} = A_i \sqrt{P_i^{SOP^2} + Q_i^{SOP^2}} \tag{5}$$

$$P_j^{SOP,L} = A_j \sqrt{P_j^{SOP^2} + Q_j^{SOP^2}} \tag{6}$$

$$\xi_i^{min} S_i \leqslant Q_i^{SOP} \leqslant \xi_i^{max} S_i,\ \xi_j^{min} S_j \leqslant Q_j^{SOP} \leqslant \xi_j^{max} S_j \tag{7}$$

$$\sqrt{P_i^{SOP^2} + Q_i^{SOP^2}} \leqslant S_i,\ \sqrt{P_j^{SOP^2} + Q_j^{SOP^2}} \leqslant S_j \tag{8}$$

where subscripts i and j indicate the indexes of the nodes to which the installed SOP is connected. P_i^{SOP} and P_j^{SOP} are the active power injection to buses i and j of the SOP, respectively. Similarly, Q_i^{SOP} and Q_j^{SOP} are the reactive power injection to buses i and j of the SOP, respectively. $P_i^{SOP,L}$ and $P_j^{SOP,L}$ are the losses of the SOP's converters connected to buses i and j, respectively. Expression (4) is the power balance constraint considering the loss of the SOPs, and constraints (5)-(6) give the formulation of the loss of the SOPs with coefficients A_i and A_j. Constraints (7) and (8) are the reactive power limits and capacity limits of the SOPs, respectively.

C. Optimal Operation of SOPs Against LAAs

In the operation model of the distribution system against the LAAs, the DSO needs to coordinate the operation of the SOPs in the system so that the network constraints can be met under the attacks. The optimization model of the network operation with SOPs is presented as follows.

$$\min \sum_{i\in\mathcal{N}}\left(r_i\frac{P_i^2+Q_i^2}{V_{i'}^2}\right)+\sum_{\psi\in\Psi}\sum_{i\in\mathcal{N}_\psi}P_{\psi,i}^{SOP,L} \tag{9}$$

Subject to

$$\sum_{i''\in\mathcal{N}_i}P_{i''}=P_i-r_iI_i-(P_i^L+P_i^A)+\sum_{\psi\in\Psi_i}P_{\psi,i}^{SOP} \quad \forall i\in\mathcal{N} \tag{10}$$

$$\sum_{i''\in\mathcal{N}_i}Q_{i''}=Q_i-x_iI_i-(Q_i^L+Q_i^A)+\sum_{\psi\in\Psi_i}Q_{\psi,i}^{SOP} \quad \forall i\in\mathcal{N} \tag{11}$$

$$V_i^2=V_{i'}^2-2\left(r_iP_i+x_iQ_i\right)+\left(r_i^2+x_i^2\right)I_i \quad \forall i\in\mathcal{N} \tag{12}$$

$$P_i^2+Q_i^2\leqslant I_iU_{i'} \quad \forall i\in\mathcal{N} \tag{13}$$

$$U_i=V_i^2 \quad \forall i\in\mathcal{N} \tag{14}$$

$$\sqrt{P_i^2+Q_i^2}\leqslant S_i^{max} \quad \forall i\in\mathcal{N} \tag{15}$$

$$V^{min}\leqslant V_i\leqslant V^{max} \quad \forall i\in\mathcal{N} \tag{16}$$

$$P_{\psi,i}^{SOP}+P_{\psi,i}^{SOP,L}+P_{\psi,j}^{SOP}+P_{\psi,j}^{SOP,L}=0 \quad i,j\in\mathcal{N}_\psi,\ \forall\psi\in\Psi \tag{17}$$

$$\sqrt{P_{\psi,i}^{SOP^2}+Q_{\psi,i}^{SOP^2}}\leqslant\frac{P_{\psi,i}^{SOP,L}}{A_{\psi,i}} \quad \forall i\in\mathcal{N}_\psi,\forall\psi\in\Psi \tag{18}$$

$$\xi_{\psi,i}^{min}S_{\psi,i}\leqslant Q_{\psi,i}^{SOP}\leqslant\xi_{\psi,i}^{max}S_{\psi,i} \quad \forall i\in\mathcal{N}_\psi,\forall\psi\in\Psi \tag{19}$$

$$\sqrt{P_{\psi,i}^{SOP^2}+Q_{\psi,i}^{SOP^2}}\leqslant S_{\psi,i} \quad \forall i\in\mathcal{N}_\psi,\forall\psi\in\Psi \tag{20}$$

$$S_{\psi,i}=\arg\min\mathcal{F}_{SOP} \quad \forall i\in\mathcal{N}_\psi,\forall\psi\in\Psi \tag{21}$$

where $\{P_i,Q_i,V_i,I_i,U_i,P_{\psi,i}^{SOP},P_{\psi,i}^{SOP,L},Q_{\psi,i}^{SOP}\}$ are variables in the optimization problem.

The objective of the operation model as (9) aims to minimize the total loss in the distribution network. The first term of (9) is the loss in the branches of the network, and the second term is the loss of the converters in the SOPs. The original DistFLow model as (1)-(3) is non-convex. Thus, the DistFlow model is reformulated into a second-order cone programming (SOCP) model [32], [36]. Constraints (10)-(14) give the SOCP formulation of the DistFlow model. As shown in constraints (10) and (11), the loads in the network may be altered by successful LAA attempts. Thus, the operation of the SOPs should mitigate the impacts of the altered demand in the attacks while satisfying the network constraints of the grid. Constraints (15)-(16) guarantee the network constraints of the distribution system operation. The model of the SOP operation as (4)-(8) is also non-convex. Similarly, a SOCP reformulation of the SOP operation model is applied [14]. Constraints (17)-(20) show the SOCP model of the SOP operation. The SOCP reformulation in (17)-(20) relaxes the equality constraints (5) and (6) with the inequality constraint (18). Suppose $P_{\psi,i}^{SOP,L}$ is a solution when (18) is not binding. It can be expressed as $P_{\psi,i}^{SOP,L}=A_{\psi,i}\sqrt{P_{\psi,i}^{SOP^2}+Q_{\psi,i}^{SOP^2}}+\Delta$, where $\Delta>0$. As $P_{\psi,i}^{SOP,L}\geqslant 0$ according to (18), it can be derived from (17) that $P_{\psi,i}^{SOP}\cdot P_{\psi,j}^{SOP}\leqslant 0$. When $P_{\psi,i}^{SOP}\geqslant 0$, it means the SOP draws active power from node i. When $P_{\psi,i}^{SOP}\leqslant 0$, it means the SOP injects active power to node i. Without loss of generality, assume $P_{\psi,i}^{SOP}\leqslant 0$ and $P_{\psi,j}^{SOP}\geqslant 0$. As $-P_{\psi,i}^{SOP}=P_{\psi,i}^{SOP,L}+P_{\psi,j}^{SOP,L}+P_{\psi,j}^{SOP}=A_{\psi,i}\sqrt{P_{\psi,i}^{SOP^2}+Q_{\psi,i}^{SOP^2}}+\Delta+P_{\psi,j}^{SOP,L}+P_{\psi,j}^{SOP}$, it can easily be derived that the value of $\left|P_{\psi,i}^{SOP}\right|$ decreases when Δ decreases, which means more active power is drawn by the SOP at node i. Then the active power flow $P_{i'}$ in the upstream branches of node i increases, and the voltages $V_{i'}$ of the nodes i' in the same branches of node i decrease. As a result, the value of the first term in the objective function (9) decreases. Meanwhile, a smaller Δ reduces $P_{\psi,i}^{SOP,L}$ and the value of the second term in the objective function (9). Therefore, the objective of the optimization can always be improved by reducing Δ when constraint (18) is not binding. Constraint (18) is binding when the optimal solution is reached. Thus, the SOCP reformulation (17)-(20) will result in the optimal solution of the original model with equality constraints (5) and (6). Intuitively, the increased $P_{\psi,i}^{SOP}$ when (18) is not binding can be viewed as an extra load at node i, which will further increase the burden of the network. Therefore, the optimal solution is reached when constraint (18) is binding. As indicated by (21), the capacity of the SOPs is determined by the solution of the optimization problem $\mathcal{F}_{SOP}$ for the SOP installation and sizing strategy against LAAs. The detailed formulation of $\mathcal{F}_{SOP}$ is presented in the following subsection.

In this study, the SOPs are dispatched after an attack is launched and the load at the compromised bus is altered. The set-points are determined and sent by the DSO to the SOP controllers. In the LAAs, the attackers only compromise and gain the control of the RCL in the consumption sector. The control and communication of the DSO to the local controllers in the distribution system are assumed to be secured in this paper.

D. Chance-Constrained Installation Model of SOPs Against LAAs

In order to determine the optimal installation and sizing strategies of the SOPs in distribution systems to mitigate the

impacts of LAAs, a chance-constrained optimization model is proposed in this study. The chance-constrained optimization model is presented as follows.

$$\min \mathcal{F}_{SOP} = \sum_{\psi \in \widetilde{\Psi}} \left(\alpha z_\psi + \beta \sum_{i \in \mathcal{N}_\psi} S_{\psi,i} \right) \tag{22}$$

Subject to

$$\sum_{i'' \in \mathcal{N}_i} P_{i'',a,\omega} = P_{i,a,\omega} - r_i I_{i,a,\omega} - \left(P^L_{i,\omega} + P^A_{i,a,\omega}\right) + \sum_{\psi \in \widetilde{\Psi}_i} P^{SOP}_{\psi,i,a,\omega} \quad \forall i \in \mathcal{N}, \forall a \in \mathcal{A}, \forall \omega \in \Omega \tag{23}$$

$$\sum_{i'' \in \mathcal{N}_i} Q_{i'',a,\omega} = Q_{i,a,\omega} - x_i I_{i,a,\omega} - \left(Q^L_{i,\omega} + Q^A_{i,a,\omega}\right) + \sum_{\psi \in \widetilde{\Psi}_i} Q^{SOP}_{\psi,i,a,\omega} \quad \forall i \in \mathcal{N}, \forall a \in \mathcal{A}, \forall \omega \in \Omega \tag{24}$$

$$V^2_{i,a,\omega} = V^2_{i',a,\omega} - 2\left(r_i P_{i,a,\omega} + x_i Q_{i,a,\omega}\right) + \left(r_i^2 + x_i^2\right) I_{i,a,\omega} \quad \forall i \in \mathcal{N}, \forall a \in \mathcal{A}, \forall \omega \in \Omega \tag{25}$$

$$P^2_{i,a,\omega} + Q^2_{i,a,\omega} \leqslant I_{i,a,\omega} U_{i',a,\omega} \quad \forall i \in \mathcal{N}, \forall a \in \mathcal{A}, \forall \omega \in \Omega \tag{26}$$

$$U_{i,a,\omega} = V^2_{i,a,\omega} \quad \forall i \in \mathcal{N}, \forall a \in \mathcal{A}, \forall \omega \in \Omega \tag{27}$$

$$P^{SOP}_{\psi,i,a,\omega} + P^{SOP,L}_{\psi,i,a,\omega} + P^{SOP}_{\psi,j,a,\omega} + P^{SOP,L}_{\psi,j,a,\omega} = 0 \quad i,j \in \mathcal{N}_\psi, \forall \psi \in \widetilde{\Psi}, \forall a \in \mathcal{A}, \forall \omega \in \Omega \tag{28}$$

$$\sqrt{P^{SOP^2}_{\psi,i,a,\omega} + Q^{SOP^2}_{\psi,i,a,\omega}} \leqslant \frac{P^{SOP,L}_{\psi,i,a,\omega}}{A_{\psi,i}} \quad \forall i \in \mathcal{N}_\psi, \forall \psi \in \widetilde{\Psi}, \forall a \in \mathcal{A}, \forall \omega \in \Omega \tag{29}$$

$$\xi^{min}_{\psi,i} S_{\psi,i} \leqslant Q^{SOP}_{\psi,i,a,\omega} \leqslant \xi^{max}_{\psi,i} S_{\psi,i} \quad \forall i \in \mathcal{N}_\psi, \forall \psi \in \widetilde{\Psi}, \forall a \in \mathcal{A}, \forall \omega \in \Omega \tag{30}$$

$$\sqrt{P^{SOP^2}_{\psi,i,a,\omega} + Q^{SOP^2}_{\psi,i,a,\omega}} \leqslant S_{\psi,i} \quad \forall i \in \mathcal{N}_\psi, \forall \psi \in \widetilde{\Psi}, \forall a \in \mathcal{A}, \forall \omega \in \Omega \tag{31}$$

$$S_{\psi,i} \leqslant M z_\psi \quad z_\psi \in \{0,1\}, \forall i \in \mathcal{N}_\psi, \forall \psi \in \widetilde{\Psi} \tag{32}$$

$$\mathbb{P}\left\{ \begin{matrix} \sqrt{P^2_{i,a,\omega} + Q^2_{i,a,\omega}} \leqslant S^{max}_i, \\ V^{min} \leqslant V_{i,a,\omega} \leqslant V^{max} \end{matrix} \quad \forall i \in \mathcal{N} \right\} \geqslant 1 - \varepsilon \quad \forall a \in \mathcal{A} \tag{33}$$

where $\{P_{i,a,\omega}, Q_{i,a,\omega}, V_{i,a,\omega}, I_{i,a,\omega}, U_{i,a,\omega}, P^{SOP}_{\psi,i,a,\omega}, P^{SOP,L}_{\psi,i,a,\omega}, Q^{SOP}_{\psi,i,a,\omega}, z_\psi, S_{\psi,i}\}$ are variables in the optimization problem.

The objective of the operation model as (22) minimizes the total cost of the SOP installation in the distribution system. The first term of (22) is the fixed cost for each SOP installation, and the second term is the proportional cost to the capacities of the installed SOPs. Constraints (23)-(27) are the SOCP formulation of the DistFlow model. Expressions (28)-(31) are the SOP operation constraints. Constraint (32) limits the capacities of the SOPs according to the installation decisions. When the installation decision variable $z_\psi = 1$, it means the SOP is installed. Otherwise, $z_\psi = 0$.

Constraint (33) is the joint chance constraint of the optimization model. It enforces the constraint that the probability of network constraint violations is lower than the predefined confidence level coefficient ε for any bus in the distribution system is compromised in the LAAs. In other words, the probability of the system operation being able to adequately mitigate the impacts of the LAAs on the distribution system must be higher than the predefined confidence level $1-\varepsilon$. The chance constraint (33) in the original form cannot be solved directly. In order to solve the optimization with off-the-shelf solvers, (33) can be reformulated as (34)-(37) below.

$$\sqrt{P^2_{i,a,\omega} + Q^2_{i,a,\omega}} \leqslant S^{max}_i + M u_\omega \quad \forall i \in \mathcal{N}, \forall a \in \mathcal{A}, \forall \omega \in \Omega \tag{34}$$

$$V_{i,a,\omega} \leqslant V^{max} + M u_\omega \quad \forall i \in \mathcal{N}, \forall a \in \mathcal{A}, \forall \omega \in \Omega \tag{35}$$

$$V_{i,a,\omega} \geqslant V^{min} - M u_\omega \quad \forall i \in \mathcal{N}, \forall a \in \mathcal{A}, \forall \omega \in \Omega \tag{36}$$

$$\sum_{\omega \in \Omega} \pi_\omega u_\omega \leqslant \varepsilon \quad u_\omega \in \{0,1\} \tag{37}$$

When $u_\omega = 0$, constraints (34)-(36) have exactly the same expressions as the network constraints in the original chance constraint (33). Thus, the network constraints are enforced. When $u_\omega = 1$, it is easy to find that the network constraints in the original chance constraint (33) are relaxed by (34)-(36). Finally, constraint (37) guarantees that the total probability of the relaxed scenarios is lower than the predefined confidence level coefficient ε. Thus, the original chance constraint (33) is enforced by constraints (34)-(37).

The optimization model (9) subject to (10)-(21) in Section III-C is the operation model of the DSO with the installed SOPs in the distribution network based on the solution of the proposed optimization model presented in Section III-D. The optimization model (22) subject to (23)-(33) in Section III-D is the optimization model for the optimal strategy of SOP installation against potential LAAs on the distribution network. The later model aims to keep the feasibility of the former one in the face of potential LAAs with an acceptable confidence level.

In this paper, it is assumed that the attacker will be able to switch on the vulnerable RCL when compromising the target bus in the network. The RCL connected to the compromised target bus of the LAAs is considered stochastic (e.g., EVs). Thus, with different attack policies and RCL scenarios, the impacts of the LAAs on the distribution system vary. The attacker may select the most damaging attack policy when performing the LAA. The proposed SOP installation and sizing model covers all the attack policies (including the worst-case one) in each RCL scenario to maintain the operation of the DSO with the installed SOPs. Thus, the confidence level of the network operation against the LAAs is achieved.

The chance-constrained programming method with chance constraint (33) is applied in this paper. Robust optimization is another approach to provide conservative and robust solutions of the problem. However, robust optimization may result in highly conservative solutions or even infeasibility in certain cases. Thus, a chance-constrained model is proposed for the optimal strategies of the SOP installation and sizing in this

study. The probability of network constraint violation with LAAs is kept under an acceptably low level by the proposed model. The proposed model provides a robust enough and feasible solution in the cases when the budget and resource of the system are limited which need to be considered and optimized, and the cases when robust optimization cannot achieve feasible solutions. The proposed model aims to keep the probability of network constraint violation with LAAs under an acceptably low level by the DSO. Meanwhile, it should be noted that if the highest level of network operation security is preferred by the DSO, the confidence level coefficient in the proposed model ε can be set as zero. In this case, the proposed model is equivalent to the case with robust optimization in which the network constraints under attack in all the scenarios will be respected.

While the operation of the SOPs is considered in the model, the proposed SOP installation model aims to provide the optimal SOP installation and sizing strategy against potential LAAs on the distribution network. In practice, it is generally not feasible for the DSO to install the SOP between any two nodes of the grid arbitrarily due to practical engineering reasons, e.g., spatial constraints. Certain possible locations for the SOP installation will be selected and assumed before the installation strategy is determined. Thus, the location candidates of the SOP installation are assumed to be known in the proposed model. Meanwhile, although placing the SOPs at the nodes close to the location of the controllable loads in the network can mitigate the impacts of the LAAs more directly, however, the placement of SOPs is usually subject to practical constraints and only certain places are feasible as discussed above. The proposed model aims to install the SOPs optimally considering all the selected feasible site candidates for the SOP installation.

IV. Distributionally Robust Chance-Constrained Modeling

In practice, the estimated probability distribution obtained from the empirical data may not perfectly reflect the true probability distribution of the scenarios. In order to robustize the chanced-constrained SOP installation model against the uncertainty of the empirical probability measure, a Wasserstein metric based DRCC model is proposed.

A. Ambiguity Set with Wasserstein Distance

The ambiguity set $\mathcal{D}$ of the DRCC model is defined based on the Wasserstein distance. The Wasserstein distance is a well accepted metric to construct ambiguity set for its strong out-of-sample performance. The formulation is introduced below. The Wasserstein distance between two probability measures $d_W(\boldsymbol{\pi}_1, \boldsymbol{\pi}_2) : \mathcal{M}(\Xi) \times \mathcal{M}(\Xi) \to \mathbb{R}$ is defined as (38) [21].

$$d_W(\boldsymbol{\pi}_1, \boldsymbol{\pi}_2) = \inf_{\gamma \in \Gamma(\boldsymbol{\pi}_1, \boldsymbol{\pi}_2)} \int_{\Xi^2} \|\boldsymbol{\omega}_1 - \boldsymbol{\omega}_2\| \, \mathrm{d}\gamma(\boldsymbol{\omega}_1, \boldsymbol{\omega}_2) \quad (38)$$

where Ξ is the support of the two probability measures; $\mathcal{M}(\Xi)$ is the set of all the distributions with support Ξ; Γ is the set of all the joint distributions with marginal distributions $\boldsymbol{\pi}_1$ and $\boldsymbol{\pi}_2$. Then the Wasserstein distance based ambiguity set $\mathcal{D}$ can be defined via (39).

$$\mathcal{D} = \{\boldsymbol{\pi} \in \mathcal{M}(\Xi) \mid d_W(\boldsymbol{\pi}, \boldsymbol{\varpi}) \leqslant \rho\} \quad (39)$$

As shown above, the Wasserstein distance from any distribution in the ambiguity set $\mathcal{D}$ to the estimated distribution $\boldsymbol{\varpi}$ is constrained by ρ. Thus, the ambiguity set $\mathcal{D}$ can be viewed as the Wasserstein ball with radius ρ, the center of which is the estimated distribution $\boldsymbol{\varpi}$. The Wasserstein distance-based ambiguity set can provide an upper confidence bound without assigning probability weights, has good out-of-sample performance and has a series of nice characteristics [21], [23]. Thus, in this study, the ambiguity set is constructed based on the Wasserstein distance.

B. Distributionally Robust Chance-Constrained Model

In the distributionally robust model, the chance constraint (33) in the original model is replaced by constraint (40) as follows.

$$\min_{\boldsymbol{\pi} \in \mathcal{D}} \mathbb{P}\left\{ \begin{array}{l} \sqrt{P_{i,a,\omega}^2 + Q_{i,a,\omega}^2} \leqslant S_i^{max}, \quad \forall i \in \mathcal{N} \\ V^{min} \leqslant V_{i,a,\omega} \leqslant V^{max} \end{array} \right\} \geqslant 1 - \varepsilon \quad \forall a \in \mathcal{A} \quad (40)$$

Similar to the reformulation of (33) by (34)-(37), constraint (40) can be reformulated as (34)-(36) and (41) as presented below.

$$\max_{\boldsymbol{\pi} \in \mathcal{D}} \left\{ \sum_{\omega \in \Omega} \pi_\omega u_\omega \right\} \leqslant \varepsilon \quad u_\omega \in \{0, 1\} \quad (41)$$

In order to formulate the ambiguity set $\mathcal{D}$ explicitly in the optimization, the Wasserstein distance needs to be calculated in a closed form. According to the definition of the Wasserstein distance, an optimization model is constructed to calculate the Wasserstein distance of a distribution $\boldsymbol{\pi}$ from the estimated distribution $\boldsymbol{\varpi}$ as follows.

$$d_W(\boldsymbol{\pi}, \boldsymbol{\varpi}) = \min \sum_{\omega \in \Omega} \sum_{\omega' \in \Omega} d_{\omega,\omega'} \lambda_{\omega,\omega'} \quad (42)$$

Subject to

$$0 \leqslant \lambda_{\omega,\omega'} \leqslant 1 \quad \forall \omega \in \Omega, \forall \omega' \in \Omega \quad (43)$$

$$\sum_{\omega \in \Omega} \lambda_{\omega,\omega'} = \varpi_{\omega'} \quad \forall \omega' \in \Omega \quad (44)$$

$$\sum_{\omega' \in \Omega} \lambda_{\omega,\omega'} = \pi_\omega \quad \forall \omega \in \Omega \quad (45)$$

where $d_{\omega,\omega'} = \|\boldsymbol{\omega} - \boldsymbol{\omega}'\|$. Then the proposed DRCC optimization model can be formulated as a tri-level optimization problem by minimizing (22) subject to (23)-(32), (34)-(36), and

$$\sum_{\omega \in \Omega} \pi_\omega u_\omega \leqslant \varepsilon \quad u_\omega \in \{0, 1\} \quad (46)$$

$$\pi_\omega = \arg\max \sum_{\omega \in \Omega} \pi_\omega u_\omega \quad (47)$$

Subject to

$$0 \leqslant \pi_\omega \leqslant 1 \quad \forall \omega \in \Omega \quad (48)$$

$$\sum_{\omega\in\Omega}\pi_\omega = 1 \quad \forall\omega\in\Omega \tag{49}$$

$$d_W\left(\boldsymbol{\pi},\boldsymbol{\varpi}\right) \leqslant \rho \tag{50}$$

$$d_W\left(\boldsymbol{\pi},\boldsymbol{\varpi}\right) = \arg\min \sum_{\omega\in\Omega}\sum_{\omega'\in\Omega} d_{\omega,\omega'}\lambda_{\omega,\omega'} \tag{51}$$

Subject to (43)-(45).

In the DRCC model, ω and ω' are both the indexes for the scenarios in the sample space Ω. $\boldsymbol{\omega}$ and $\boldsymbol{\omega}'$ are the realization values of scenarios ω and ω', which are the amounts of RCL at the vulnerable nodes in scenarios ω and ω' in this study. In the ambiguity set $\mathcal{D}$, all the distributions (including the estimated distribution itself) have the same support as the estimated distribution. Therefore, both ω and $\omega' \in \Omega$, and both $\boldsymbol{\omega}$ and $\boldsymbol{\omega}'$ are obtained from the sample data.

C. Solution Method

In order to solve the tri-level optimization model, a master and sub-problems algorithm is developed. First, the third-level optimization problem (51) subject to (43)-(45) is reformulated by the Karush-Kuhn-Tucker (KKT) conditions as

$$d_{\omega,\omega'}+\delta_{\omega'}+\zeta_\omega-\mu_{\omega,\omega'}+\nu_{\omega,\omega'} = 0 \quad \forall\omega\in\Omega,\forall\omega'\in\Omega \tag{52}$$

$$\mu_{\omega,\omega'} \geqslant 0 \quad \forall\omega\in\Omega,\forall\omega'\in\Omega \tag{53}$$

$$\nu_{\omega,\omega'} \geqslant 0 \quad \forall\omega\in\Omega,\forall\omega'\in\Omega \tag{54}$$

$$\mu_{\omega,\omega'}\lambda_{\omega,\omega'} = 0 \quad \forall\omega\in\Omega,\forall\omega'\in\Omega \tag{55}$$

$$\nu_{\omega,\omega'}\left(1-\lambda_{\omega,\omega'}\right) = 0 \quad \forall\omega\in\Omega,\forall\omega'\in\Omega \tag{56}$$

together with (43)-(45), where (52) is the stationarity condition in the KKT conditions of optimization problem (51) subject to (43)-(45). It shows the optimal primal point $\lambda_{\omega,\omega'}$ is a minimizer of the Lagrangian with the dual variables $\delta_{\omega'}, \zeta_\omega, \mu_{\omega,\omega'}$ and $\nu_{\omega,\omega'}$. Constraints (53)-(54) are the dual feasibility conditions, and constraints (55)-(56) are the complementary slackness conditions. With the KKT based reformulation of the third-level problem, the original tri-level optimization model is converted to an equivalent bi-level optimization model. Then, the master and sub-problems are constructed to solve the bi-level optimization model. The master-problem is defined as follows.

$$\min_{z_\psi, S_{\psi,i}, u_\omega} \sum_{\psi\in\widetilde{\Psi}}\left(\alpha z_\psi + \beta\sum_{i\in\mathcal{N}_\psi} S_{\psi,i}\right) \tag{57}$$

Subject to (23)-(32), (34)-(36), and

$$\sum_{\omega\in\Omega}\pi_\omega u_\omega \leqslant \varepsilon \quad u_\omega\in\{0,1\}, \forall\{\pi_\omega\}\in\mathcal{R}_\Omega \tag{58}$$

where $\mathcal{R}_\Omega$ is a non-empty set of distributions with support Ω. $\mathcal{R}_\Omega$ will be constructed with the solutions of the sub-problem, and the detailed process will be described in **Algorithm 1** presented below.

The sub-problem is defined as follows.

$$\max_{\pi_\omega} \sum_{\omega\in\Omega}\pi_\omega u_\omega \tag{59}$$

Subject to (43)-(45), (48)-(49), (52)-(54), and

$$\sum_{\omega\in\Omega}\sum_{\omega'\in\Omega} d_{\omega,\omega'}\lambda_{\omega,\omega'} \leqslant \rho \tag{60}$$

$$\mu_{\omega,\omega'} \leqslant M\sigma_{\omega,\omega'} \quad \forall\omega\in\Omega,\forall\omega'\in\Omega \tag{61}$$

$$\lambda_{\omega,\omega'} \leqslant M\left(1-\sigma_{\omega,\omega'}\right) \quad \forall\omega\in\Omega,\forall\omega'\in\Omega \tag{62}$$

$$\nu_{\omega,\omega'} \leqslant M\varsigma_{\omega,\omega'} \quad \forall\omega\in\Omega,\forall\omega'\in\Omega \tag{63}$$

$$1-\lambda_{\omega,\omega'} \leqslant M\left(1-\varsigma_{\omega,\omega'}\right) \quad \forall\omega\in\Omega,\forall\omega'\in\Omega \tag{64}$$

$$\sigma_{\omega,\omega'}+\varsigma_{\omega,\omega'} \leqslant 1 \quad \sigma_{\omega,\omega'},\varsigma_{\omega,\omega'}\in\{0,1\}, \ \forall\omega\in\Omega,\forall\omega'\in\Omega \tag{65}$$

where (61)-(65) is an equivalent reformulation of the complementary slackness conditions (55) and (56) to handle the non-convexity of the sub-problem. With the master and sub-problems described above, an iterative algorithm is then developed to solve the proposed DRCC optimization model. The algorithm is presented as **Algorithm 1** below.

Algorithm 1: Master and sub-problems iterations

1. Denote the estimated distribution by $\boldsymbol{\varpi}$, and set $\mathcal{R}_\Omega = \{\boldsymbol{\varpi}\}$. Denote the objective function of the master-problem by Θ_m and the objective function of the sub-problem by Θ_s.
2. Solve the master-problem and set $(\mathbf{z}^*, \mathbf{S}^*, \mathbf{u}^*) = (\{z^*_\psi\}, \{S^*_{\psi,i}\}, \{u^*_\omega\}) = \arg\min\Theta_m(\mathcal{R}_\Omega)$.
3. Solve the sub-problem and set $\boldsymbol{\pi}^* = \{\pi^*_\omega\} = \arg\max\Theta_s(\mathbf{u}^*)$.
4. If $\sum_{\omega\in\Omega}\pi^*_\omega u^*_\omega \leqslant \varepsilon$ then return $(\mathbf{z}^*, \mathbf{S}^*)$ as the solution, else append $\boldsymbol{\pi}^*$ to $\mathcal{R}_\Omega$ by setting $\mathcal{R}_\Omega = \{\mathcal{R}_\Omega, \boldsymbol{\pi}^*\}$ and go to Step 2.

The sub-problem guarantees that the solution of the algorithm satisfies the lower-level problem of the bi-level model. The master-problem ensures the optimality of the solution for the upper-level problem of the bi-level model. The stopping criteria of **Algorithm 1** guarantees that the chance constraint of the DRCC model is satisfied with the worst-case distribution in the ambiguity set $\mathcal{D}$. In the objective function of the sub-problem (59), the values of u_ω are determined by the solution of the master-problem, and u_ω act as parameters in the sub-problem. Thus, objective function (59) of the sub-problem is linear, and **Algorithm 1** can be solved directly and efficiently with the off-the-shelf solvers.

V. Case Studies

In order to validate the proposed model, case studies were conducted on a 69-bus test system. The details of the case studies are presented in this section.

A. Case Study Parameters

The test system based on the 69-bus system in the case studies is shown in Fig. 2. The data of the 69-bus test system can be obtained from the MATPOWER software package [37]. In the case studies, no loop paths in the 69-bus system are connected to keep it a radial network. The configuration of the SOP installation candidates follows the test system in [19]. Four potential SOP installations are considered. As shown in Fig. 2, they are supposed to be connected between Buses 31 and 38, 11 and 43, 50 and 57, 27 and 65, respectively. In

This article has been accepted for publication in a future issue of this journal, but has not been fully edited. Content may change prior to final publication. Citation information: DOI 10.1109/TSG.2021.3134176, IEEE Transactions on Smart Grid

the case studies, the EV charging demand connected to the network is assumed to be the RCL which are potential targets of the LAAs. As shown in the figure, ten buses are assumed to have EV charging infrastructures. The number of charging poles at each bus is listed in Table I. The maximum output of each charging pole is set as 7.2kW, which is a typical capacity of the Level-2 charging units. The EV driving patterns are obtained from the real-world driving data from the National Travel Surveys (NTS) of the Nordic area [38].

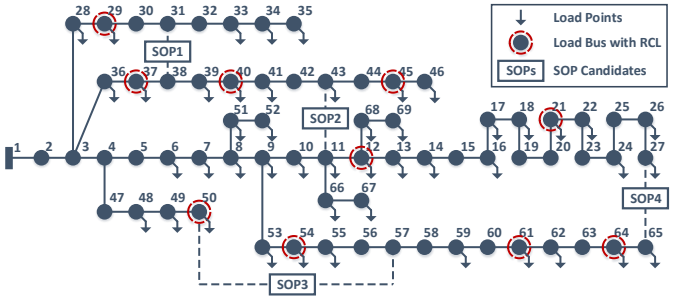

Fig. 2. 69-Bus Test System with SOPs.

TABLE I
NUMBER OF CHARGING POLES AT EACH BUS

Buses	Number of Charging Poles
Buses 21, 37, 40, 54	40
Buses 12, 29, 45, 50, 64	60
Bus 61	80

In the case studies, the real-world daily driving behavior data from the Danish NTS dataset was used to generate the scenarios. 24000 daily driving behavior records in weekdays from the NTS were used to generate 1000000 scenarios with the bootstrap method. The bootstrap method is a well-established and widely applied resampling technique used to estimate the statistic characteristics on a population by sampling a dataset with replacement. Interested readers are referred to references [39], [40]. Meanwhile, another separate 10187 records of weekdays driving behaviors from the NTS dataset were used in the out-of-sample test. In each scenario, the original charging scheduling of EVs without LAAs is determined by a TOU charging scheme [41]. The daily load curve and corresponding TOU in the case studies are shown in Figs. 3 and 4, respectively.

The loading levels of the network with the TOU-based EV charging demand without the presence of LAAs are shown in Fig. 5. As shown in the figure, the loading of the network is kept below the limits in the peak, flat and valley periods with the TOU charging scheme when there are no LAAs.

The key parameters of the model in the case studies are listed in Table II. Meanwhile, in practice, the two converters in the back-to-back topology generally have the same capacity. Therefore, it is assumed that the two converters in each SOP have the same capacity in the case studies.

In this study, the proposed DRCC model was solved using the proposed **Algorithm 1** in Section IV-C. Both the master and sub-problems in the algorithm can be solved directly

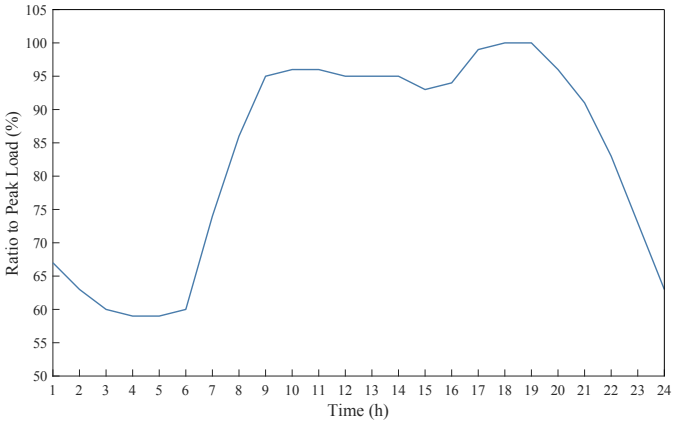

Fig. 3. Daily Load Curve in the Case Studies.

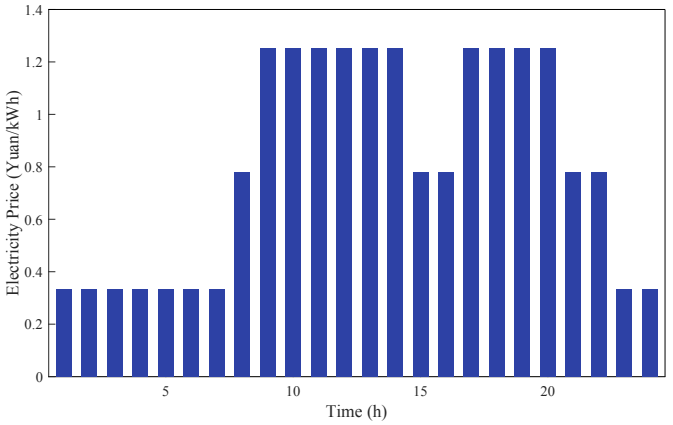

Fig. 4. TOU Electricity Prices for EV Charging.

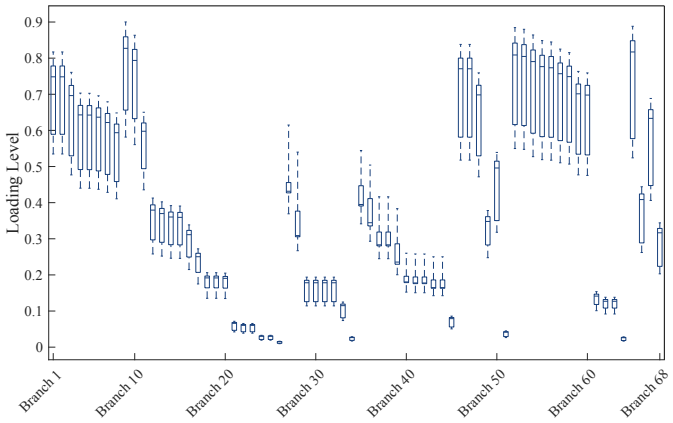

Fig. 5. Loading Levels without LAAs.

with off-the-shelf solvers. In the case study, the models were solved with CPLEX on a laptop with Intel Core i5 CPU (1.60-3.90GHz) and 12GB RAM.

B. SOP Installation and Sizing Strategies

The results of the SOP installation and sizing strategies with the proposed DRCC model are shown in Table III. The results with the generic chance-constrained (CC) and robust optimization (RO) models are also listed in the table

This article has been accepted for publication in a future issue of this journal, but has not been fully edited. Content may change prior to final publication. Citation information: DOI 10.1109/TSG.2021.3134176, IEEE Transactions on Smart Grid

TABLE II
KEY PARAMETERS IN CASE STUDIES

Parameter	Value
SOP Loss Coefficient ($A_{\psi,i}$)	0.02
SOP Reactive Power Limits ($\xi_{\psi,i}^{max}, \xi_{\psi,i}^{min}$)	$0.8, -0.8$
System Voltage Limits (V^{max}, V^{min})	1.05, 0.95 p.u.
Chance-Constrained Confidence Coefficient (ε)	0.05
Wasserstein Distance Limit (ρ)	0.001
Cost Coefficient of SOP Installation (α)	\$100K/unit
Cost Coefficient of SOP Installation (β)	\$100/kW

for comparison. With both the DRCC and CC models, only three SOPs are installed in the networks while four SOPs are installed in the result of the RO model. Meanwhile, the total capacity of the SOPs with the RO model is clearly higher than the result of the DRCC model. In contrast, the capacity of the SOPs in the result of the CC model is slightly lower than the result of the DRCC model. As a result, the costs of the SOP installation with the DRCC, CC and RO models are about \$420K, \$414K and \$540K, respectively. While the difference between the costs with the DRCC and CC models is marginal, the cost with the RO model is significantly higher, which is an about 30% raise compared with the other two models. The characteristics of the solutions from the three models are as expected. The RO model merely considers and optimizes the worst-case scenario. Therefore, it results in the most conservative solution as shown in the table. It should also be noted that the RO model may result in infeasibility of the problem is certain cases. The generic CC model relies on the estimated distribution of the scenarios and does not provide robustness against the ambiguity of the probability distribution for the chance constraint. Thus, the generic CC model gives the most optimistic solution. In contrast, the proposed DRCC model considers the ambiguity of the probability distribution and searches for the robust solution given that the estimated distribution of the scenarios may not be perfectly correct. The Wasserstein distance based ambiguity set formulation enables the proposed DRCC model to provide necessary robustness in the solution and guarantee the satisfaction of the chance constraint. Thus, as an intermediate approach between the RO and generic CC models, the proposed DRCC model provides robustness in the solution without being overly conservative.

TABLE III
SOP INSTALLATION AND SIZING SOLUTIONS WITH DIFFERENT MODELS

SOPs Installation	SOP 1	SOP 2	SOP 3	SOP 4
DRCC Installation Decision	Y	N	Y	Y
Converter Capacity (kW)	241	NA	127	232
CC Installation Decision	Y	N	Y	Y
Converter Capacity (kW)	222	NA	121	227
RO Installation Decision	Y	Y	Y	Y
Converter Capacity (kW)	270	11	166	255

The computation time of the DRCC, CC and RO models in the case studies is about 2514s, 1004s and 171s, respectively.

C. Out-of-Sample Analysis

In the case studies, the confidence level requirement is set to be 0.95, which means the probability of network constraint violations under LAAs is required to be lower than 0.05 with the installed SOPs. In other words, the probability of interruptions in the distribution system due to the LAAs is less than 0.05. When the distribution of the scenarios is accurate, the confidence level is guaranteed by both the proposed DRCC and generic CC models. However, when the ambiguity of the probability distribution is considered, the confidence level is not guaranteed by the generic CC model any more. In order to illustrate the robustness of the proposed DRCC model against the ambiguity of the probability distribution and its out-of-sample performance, the proposed Wasserstein distance based DRCC model and the generic CC model are tested in the out-of-sample analysis. As mentioned, the scenarios of the out-of-sample tests were generated with a set of independent driving records from the NTS other than the data used to solve the optimization models. Ten out-of-sample tests were conducted, and the results of the tests are shown in Fig. 6.

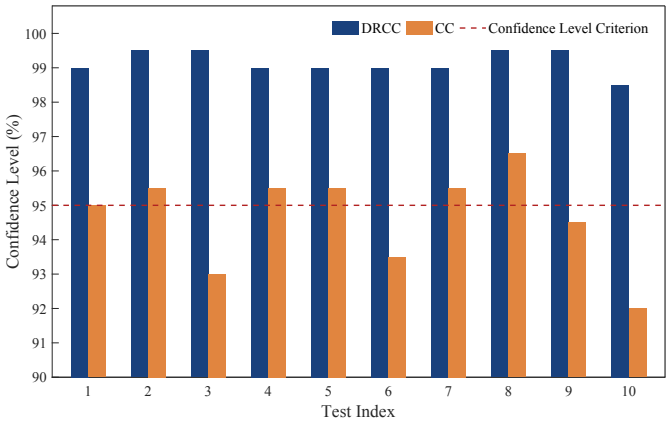

Fig. 6. Confidence Levels with DRCC and CC Models in Out-of-Sample Tests.

As shown in the figure, with the ambiguity of the distribution, the confidence level with the solution of the generic CC model is not guaranteed any more and drops below the predefined criteria in four of the tests. Thus, the generic CC model shows weak robustness to the ambiguity of the probability distribution. In contrast, the confidence level with the solution of the proposed DRCC model remains well above the criteria in all the tests. The confidence level keeps a satisfying level above 98% in all the tests, and proves the robustness of the proposed Wasserstein distance based DRCC model against the ambiguity of the probability distribution and its strong out-of-sample performance. Thus, even when the estimated probability distribution is not completely accurate in practice, the DRCC model can still maintain the required confidence level of the solution.

D. Sensitivity Analysis

The chance-constrained confidence coefficient ε and Wasserstein distance limit ρ are the key parameters in the models. The chance-constrained confidence coefficient ε sets

This article has been accepted for publication in a future issue of this journal, but has not been fully edited. Content may change prior to final publication. Citation information: DOI 10.1109/TSG.2021.3134176, IEEE Transactions on Smart Grid

the confidence level criteria of the solution, and Wasserstein distance limit ρ determines the robustness of the DRCC model against the ambiguity of distributions. A sensitivity analysis on the two parameters was conducted to show their impacts on the solution of the DRCC model.

Figs. 7 and 8 show the cost of SOP installation and average confidence level in the out-of-sample tests with different chance-constrained confidence coefficient ε. When the value of ε increases, it means the DSO can tolerate a lower confidence level of the solution. As a result, the cost for the SOP installation decreases and a less robust solution is obtained. However, as shown in Fig. 8, the proposed Wasserstein distance based DRCC model still shows a strong out-of-sample performance and well guarantees the required confidence level with the increased ε setting.

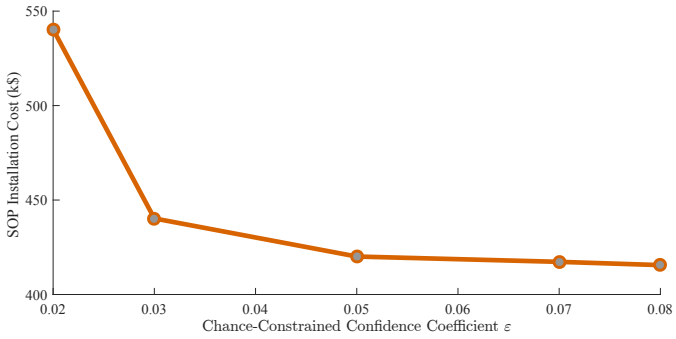

Fig. 7. SOP Installation Cost with Different ε.

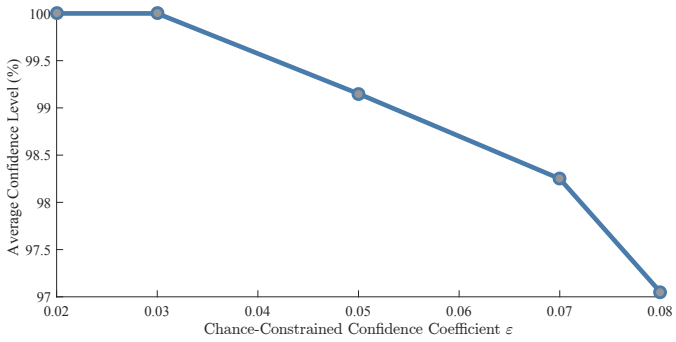

Fig. 8. Average Confidence Level in Out-of-Sample Tests with Different ε.

Figs. 9 and 10 show the cost of SOP installation and average confidence level in the out-of-sample tests with different Wasserstein distance limit ρ. A higher ρ means a larger ambiguity set and higher robustness against the ambiguity is required. Therefore, as shown in the figures, the cost for the SOP installation increases and higher robustness in the out-of-sample tests is obtained by the solution when ρ increases.

E. SOP Operation Strategy Against LAAs

In order to illustrate the performance of the proposed operation model in mitigating the impacts of the LAAs on the distribution system, the proposed SOP operation model under the LAA scenarios are tested.

In this paper, it is assumed that the attacker will be able to switch on the vulnerable RCL when compromising the

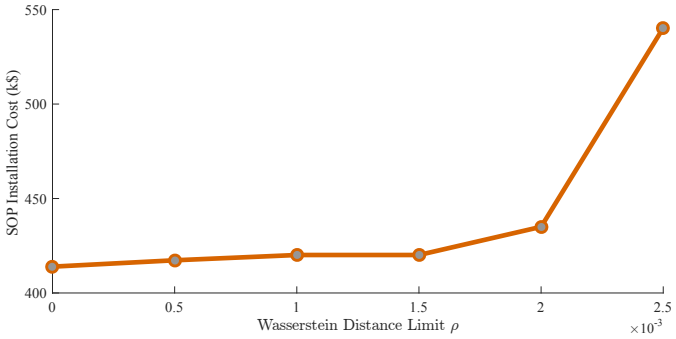

Fig. 9. SOP Installation Cost with Different ρ.

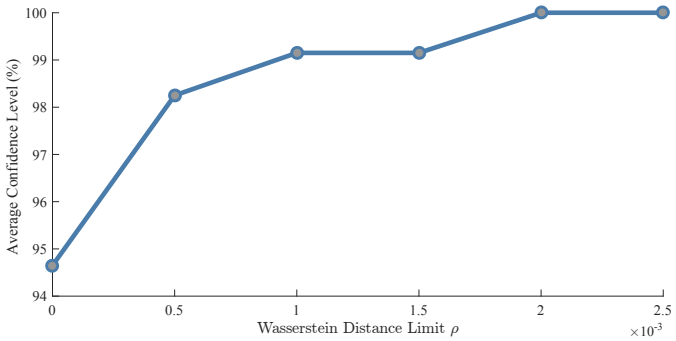

Fig. 10. Average Confidence Level in Out-of-Sample Tests with Different ρ.

target bus in the network. In the case study, it is assumed that the attacker gains the control of the EV charging when the charging infrastructure at the target bus is compromised. For instance, when the charging system at Bus 12 is compromised by the attacker, he/she can turn on the charging of all the idle EVs that are plugged in the charging poles at the charging power limit simultaneously. In this case, the default protections of the EV chargers will not be triggered. However, the network constraints of the distribution system may be violated due to the sudden peak demand, and overloading and under-voltage problems can be caused by the malicious attack action. It should be noted that the vulnerable RCL is assumed to be stochastic in the LAA scenarios in the proposed model. In the case studies, it is assumed that the attacker can switch on the charging of all the idle EVs connected to the compromised buses in the LAA attacks. The numbers of the idle EVs connected to the compromised buses in the scenarios are stochastic in the case studies.

Fig. 11 shows the ratio of the apparent power to the limits of the heavy loaded branches in the distribution system under LAAs without SOPs. Without the installation of SOPs, overloads of branches in the distribution system occur. As shown in Fig. 11, without the SOPs, the apparent power in a series of branches exceeds the limit in the cases when Buses 12, 21, 29, 45, 50, 61 or 64 is compromised. Especially when the RCL at Bus 12 or 29 are compromised, the apparent power of the overloaded upstream branches is well above the limit. As a result, load shedding will be inevitable in these cases.

In contrast, the cases with the proposed SOP operation model under the LAAs are shown in Fig. 12. The installation

This article has been accepted for publication in a future issue of this journal, but has not been fully edited. Content may change prior to final publication. Citation information: DOI 10.1109/TSG.2021.3134176, IEEE Transactions on Smart Grid

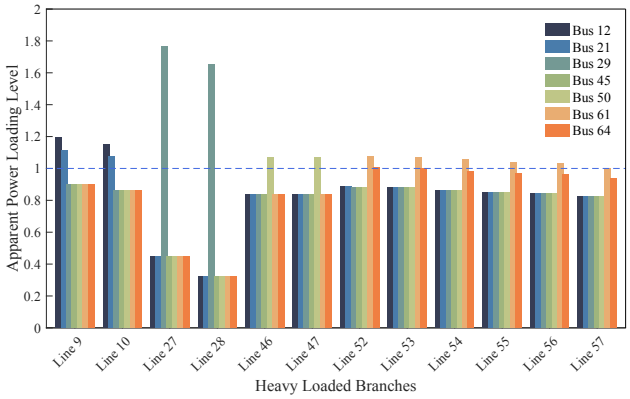

Fig. 11. Loading Levels of Branches under LAAs without SOPs.

decisions and capacities of the SOPs in the network are determined according to the proposed DRCC optimization model. The results of the test show that with proper operation of the SOPs in the distribution system, the overloads of the branches under LAAs in the test is eliminated. The apparent power of all the branches in the network is constrained within the limit under the LAAs with the proposed SOP installation and operation strategies.

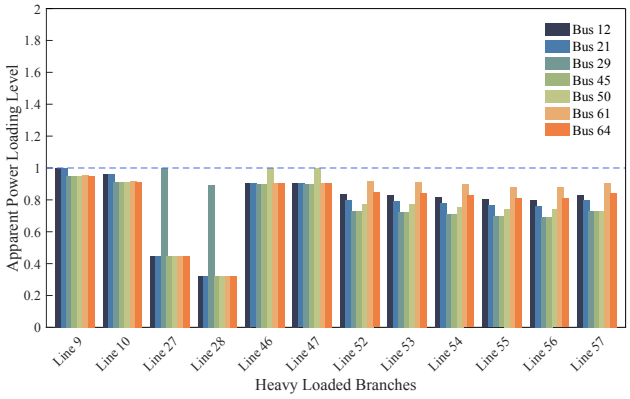

Fig. 12. Loading Levels of Branches under LAAs with SOPs.

Tables IV and V show the operation of the SOPs with the operation model to mitigate the impacts of LAAs when the RCL at Buses 12 and 29 are compromised, respectively. The power injection and losses of the SOPs with the operation model are listed in the tables.

TABLE IV
OPERATION AND LOSSES OF SOPS WITH BUS 12 COMPROMISED

Unit: kW	SOP 1	SOP 2	SOP 3	SOP 4
Active Power (P_i^{SOP})	0	NA	-109	133
Power Loss ($P_i^{SOP,L}$)	0	NA	2	5
Reactive Power (Q_i^{SOP})	0	NA	15	186
Active Power (P_j^{SOP})	0	NA	105	-142
Power Loss ($P_j^{SOP,L}$)	0	NA	3	5
Reactive Power (Q_j^{SOP})	0	NA	73	184

Further, the proposed installation and operation model of SOPs also address the voltage problem of the distribution system due to the LAAs. In the test, under-voltage issues occur in the network when Bus 61 or 64 is compromised in the LAAs. Fig. 13 shows the nodal voltages of the system under LAAs in the cases when Bus 61 and Bus 64 is compromised. As shown in the figure, Buses 60-65 have under-voltage problems when Bus 61 is compromised, and Buses 61-65 have under-voltage problems when Bus 64 is compromised without SOPs in the test. However, if the SOPs are installed, the under-voltage issues in the networks under LAAs are eliminated with the proposed SOP installation and operation strategies. The voltages of all the buses in the distribution network are well kept within the specified range.

TABLE V
OPERATION AND LOSSES OF SOPS WITH BUS 29 COMPROMISED

Unit: kW	SOP 1	SOP 2	SOP 3	SOP 4
Active Power (P_i^{SOP})	188	NA	-101	-149
Power Loss ($P_i^{SOP,L}$)	4	NA	2	5
Reactive Power (Q_i^{SOP})	40	NA	14	179
Active Power (P_j^{SOP})	-196	NA	97	139
Power Loss ($P_j^{SOP,L}$)	4	NA	3	5
Reactive Power (Q_j^{SOP})	2	NA	83	186

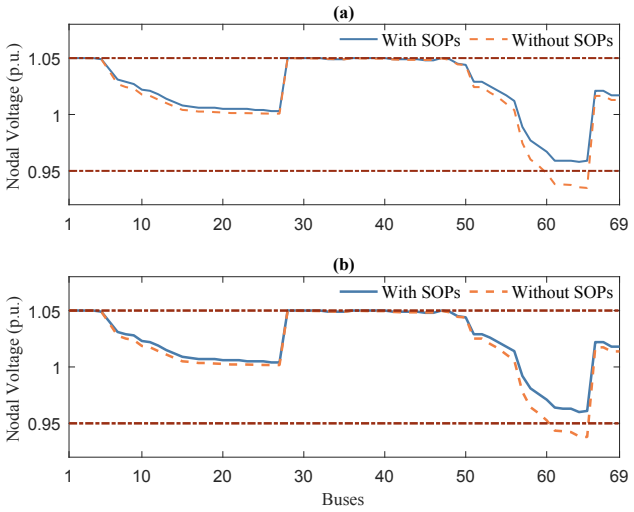

Fig. 13. Nodal Voltages under LAAs when (a) Bus 61 is compromised, (b) Bus 64 is compromised.

Tables VI and VII show the operation of the SOPs with the operation model to mitigate the impacts of LAAs when the RCL at Buses 61 and 64 are compromised, respectively. The power injection and losses of the SOPs with the operation model are listed in the tables.

In order to further demonstrate the benefits of the SOP installation in mitigating the impacts of LAAs, the distribution system reconfiguration method [42] is also applied in the LAA scenarios. Four additional loop paths on the same connection nodes of the SOP candidates are assumed in the scenarios. The loop paths are assumed to be equipped with and normally open circuit breakers. In the cases when Bus 37, 40, 54 or 45 is compromised by the LAAs, the reconfiguration method manages to maintain the normal operation of the distribution

This article has been accepted for publication in a future issue of this journal, but has not been fully edited. Content may change prior to final publication. Citation information: DOI 10.1109/TSG.2021.3134176, IEEE Transactions on Smart Grid

TABLE VI
OPERATION AND LOSSES OF SOPS WITH BUS 61 COMPROMISED

Unit: kW	SOP 1	SOP 2	SOP 3	SOP 4
Active Power (P_i^{SOP})	0	NA	-113	-152
Power Loss ($P_i^{SOP,L}$)	0	NA	2	5
Reactive Power (Q_i^{SOP})	0	NA	15	176
Active Power (P_j^{SOP})	0	NA	108	143
Power Loss ($P_j^{SOP,L}$)	0	NA	3	5
Reactive Power (Q_j^{SOP})	0	NA	67	183

TABLE VII
OPERATION AND LOSSES OF SOPS WITH BUS 64 COMPROMISED

Unit: kW	SOP 1	SOP 2	SOP 3	SOP 4
Active Power (P_i^{SOP})	0	NA	-110	-149
Power Loss ($P_i^{SOP,L}$)	0	NA	2	5
Reactive Power (Q_i^{SOP})	0	NA	15	179
Active Power (P_j^{SOP})	0	NA	105	139
Power Loss ($P_j^{SOP,L}$)	0	NA	3	5
Reactive Power (Q_j^{SOP})	0	NA	72	186

system while satisfying the network constraints. However, in the cases when Bus 12, 21, 29, 45, 50, 61 or 64 is compromised in the LAAs, the reconfiguration method fails to mitigate the impacts of the LAAs and unwanted violations of network constraints cannot be avoided by the reconfiguration. Nevertheless, with the proposed SOP installation, the impacts of LAAs can be successfully mitigated in all the cases.

F. Case Study on 141-Bus Test System

In order to further validate the proposed DRCC based SOP installation and operation model in mitigating potential LAAs, an additional case study on the 141-bus radial test system from the MATPOWER package [37] was also performed. The EV demand data is obtained in the same way as the cases on the 69-bus system. The number of charging poles at the buses in the test system is listed in Table VIII. Four potential SOP installations are considered in the test, which are supposed to be connected between Buses 59 and 105, 32 and 52, 23 and 130, 95 and 125, respectively.The key parameters in the test are the same as the values listed in the II.

TABLE VIII
NUMBER OF CHARGING POLES IN 141-BUS SYSTEM

Buses	Number of Charging Poles
Buses 20, 42, 48, 91, 125	60
Bus 25	80

The SOP installation strategy in the test is shown in IX. With the installed SOPs in the network, an out-of-sample test was conducted to validate the SOP installation and sizing solutions. The result of the out-of-sample test is shown in Fig. 14. As shown in the figure, the confidence level of the solution in mitigation the LAAs in the out-of-sample test is well maintained beyond the predefined confidence level, 95%. The proposed Wasserstein distance based model can provide satisfying out-of-sample performance and robustness to the solution of the SOP installation in mitigating the impacts of LAAs under the ambiguity of distribution.

TABLE IX
SOP INSTALLATION SOLUTION IN THE TEST ON 141-BUS SYSTEM

SOP Installation	SOP 1	SOP 2	SOP 3	SOP 4
DRCC Installation Decision	Y	N	Y	N
Converter Capacity (kW)	138	NA	280	NA

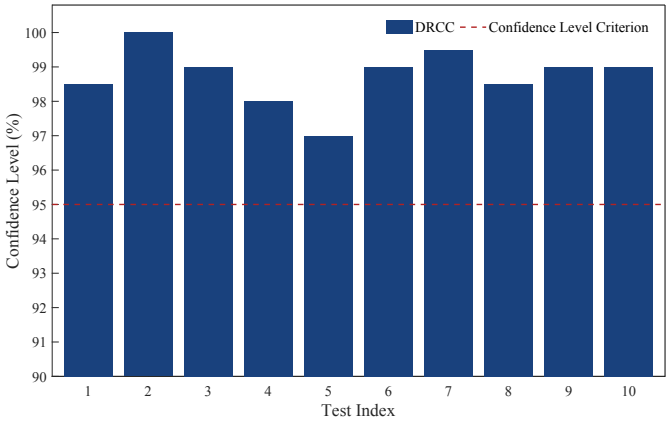

Fig. 14. Confidence Levels with DRCC Models in Out-of-Sample Tests.

G. Discussion

As shown in the case studies, the installed SOPs can provide voltage support to the network against the LAAs. In [43], a robust control principle for the Volt-Var and Volt-Watt control for smart inverters in radial grid in proposed. The results in [43] show the proposed control policy in [43] can successfully provide voltage support to the network and keep the stability. However, the research in [43] only focuses on the voltage problem in the grid while the network congestion is not addressed by the method, which is one of the major problems caused by LAAs. Meanwhile, the active power scheduling of the inverters in [43] is based on and limited by the DGs, e.g., PV. However, DG may not be available or installed for all the distribution systems, and therefore it is not in the scope of this paper. Nevertheless, an optimal coordinated control of the DG inverters and SOPs in the distribution systems with DG installation will be highly beneficial to the robustness and resilience enhancement of the grid. It is a meaningful problem which requires serious study and investigation which will be carried out in future work.

In this paper, the Wasserstein distance is applied to construct the ambiguity set and provide robustness to the solution of the chance-constrained model. As shown in the results of the case studies, the proposed Wasserstein distance based DRCC model demonstrates satisfying robustness and performance compared with the generic CC model. The results of the out-of-sample tests with real-world data show that the confidence level requirement is not guaranteed by the generic CC model with ambiguity of the distribution. In contrast, the proposed

Wasserstein distance based DRCC model can well maintain the confidence level required in the case studies. Generally, Wasserstein metric based model is believed to have strong out-of-sample performance which has been demonstrated in the case studies. However, there are also other popular alternative methods to construct the ambiguity set for the distributionally robust optimization models, e.g., moment based and divergence based methods. In the proposed model in this paper, the moment based method will lead to a non-convex model and increase the difficulty of reaching the solution. A preliminary study has been conducted on the proposed model using the divergence based method with χ divergence of order 2. The result shows the divergence based method can also provide robustness of the solution against the ambiguity of distribution. However, more serious study and analysis are needed for the application of the divergence base methods, which will be done in future work.

VI. Conclusions

This paper presents a two-stage optimization framework to mitigate the impacts of the LAAs on the distribution systems by implementing the emerging back-to-back SOPs. The proposed framework includes the optimal installation and operation strategies of the SOPs for defending the distribution systems against potential LAAs. A chance-constrained optimization model is developed to meet the confidence level requirement of the system in adequately mitigating the impacts of the LAAs. In order to ensure the robustness of the proposed model against the ambiguity of the probability distribution in practice, a Wasserstein metric based DRCC model is developed. The results of the case studies demonstrate the performance of the proposed framework. With the installation of SOPs, the proposed framework is able to mitigate the impacts of the LAAs on the distribution system. By applying the DRCC optimization technique, the proposed Wasserstein distance based model manages to satisfy the confidence level requirement under the ambiguous probability distributions. The results also show the satisfying out-of-sample performance of the proposed Wasserstein distance based DRCC model.

References

[1] "High-Impact, Low-Frequency Event Risk to the North American Bulk Power System," North American Electric Reliability Corporation (NERC), U.S. Department of Energy (DOE), Tech. Rep., June 2010.

[2] Z. Li, M. Shahidehpour, and F. Aminifar, "Cybersecurity in Distributed Power Systems," *Proceedings of the IEEE*, vol. 105, no. 7, pp. 1367–1388, 2017.

[3] N. Kshetri and J. Voas, "Hacking Power Grids: A Current Problem," *Computer*, vol. 50, no. 12, pp. 91–95, 2017.

[4] D. E. Whitehead, K. Owens, D. Gammel, and J. Smith, "Ukraine Cyber-Induced Power Outage: Analysis and Practical Mitigation Strategies," in *Proc. 70th Annual Conference for Protective Relay Engineers (CPRE)*, College Station, TX, 2017, pp. 1–8.

[5] A. H. Mohsenian-Rad and A. Leon-Garcia, "Distributed Internet-Based Load Altering Attacks Against Smart Power Grids," *IEEE Transactions on Smart Grid*, vol. 2, no. 4, pp. 667–674, 2011.

[6] S. Amini, F. Pasqualetti, and H. Mohsenian-Rad, "Dynamic Load Altering Attacks Against Power System Stability: Attack Models and Protection Schemes," *IEEE Transactions on Smart Grid*, vol. 9, no. 4, pp. 2862–2872, 2018.

[7] H. E. Brown and C. L. Demarco, "Risk of Cyber-Physical Attack via Load With Emulated Inertia Control," *IEEE Transactions on Smart Grid*, vol. 9, no. 6, pp. 5854–5866, 2018.

[8] T. Pan, S. Mishra, L. N. Nguyen, G. Lee, J. Kang, J. Seo, and M. T. Thai, "Threat From Being Social: Vulnerability Analysis of Social Network Coupled Smart Grid," *IEEE Access*, vol. 5, pp. 16 774–16 783, 2017.

[9] A. K. Marnerides, P. Smith, A. Schaeffer-Filho, and A. Mauthe, "Power Consumption Profiling Using Energy Time-Frequency Distributions in Smart Grids," *IEEE Communications Letters*, vol. 19, no. 1, pp. 46–49, 2015.

[10] J. M. Bloemink and T. C. Green, "Benefits of Distribution-Level Power Electronics for Supporting Distributed Generation Growth," *IEEE Transactions on Power Delivery*, vol. 28, no. 2, pp. 911–919, 2013.

[11] W. Cao, J. Wu, N. Jenkins, C. Wang, and T. Green, "Operating principle of Soft Open Points for electrical distribution network operation," *Applied Energy*, vol. 164, pp. 245–257, 2016.

[12] C. Long, J. Wu, L. Thomas, and N. Jenkins, "Optimal operation of soft open points in medium voltage electrical distribution networks with distributed generation," *Applied Energy*, vol. 184, pp. 427–437, 2016.

[13] A. Aithal, G. Li, J. Wu, and J. Yu, "Performance of an electrical distribution network with Soft Open Point during a grid side AC fault," *Applied Energy*, vol. 227, pp. 262–272, 2018.

[14] J. Wang, N. Zhou, C. Y. Chung, and Q. Wang, "Coordinated Planning of Converter-Based DG Units and Soft Open Points Incorporating Active Management in Unbalanced Distribution Networks," *IEEE Transactions on Sustainable Energy*, vol. 11, no. 3, pp. 2015–2027, 2020.

[15] P. Li, H. Ji, C. Wang, J. Zhao, G. Song, F. Ding, and J. Wu, "Optimal Operation of Soft Open Points in Active Distribution Networks under Three-Phase Unbalanced Conditions," *IEEE Transactions on Smart Grid*, vol. 10, no. 1, pp. 380–391, 2019.

[16] S. Ouyang, J. Liu, Y. Yang, X. Chen, S. Song, and H. Wu, "DC Voltage Control Strategy of Three-Terminal Medium-Voltage Power Electronic Transformer-Based Soft Normally Open Points," *IEEE Transactions on Industrial Electronics*, vol. 67, no. 5, pp. 3684–3695, 2020.

[17] R. Wu, L. Ran, G. Weiss, and J. Yu, "Control of a synchronverter-based soft open point in a distribution network," *The Journal of Engineering*, vol. 2019, no. 16, pp. 720–727, 2019.

[18] P. Li, H. Ji, C. Wang, J. Zhao, G. Song, F. Ding, and J. Wu, "Coordinated Control Method of Voltage and Reactive Power for Active Distribution Networks Based on Soft Open Point," *IEEE Transactions on Sustainable Energy*, vol. 8, no. 4, pp. 1430–1442, 2017.

[19] Y. Zheng, Y. Song, and D. J. Hill, "A general coordinated voltage regulation method in distribution networks with soft open points," *International Journal of Electrical Power and Energy Systems*, vol. 116, no. 105571, pp. 1–7, 2020.

[20] F. Ding, C. Wang, H. Ji, J. Wu, and P. Li, "Robust Operation of Soft Open Points in Active Distribution Networks With High Penetration of Photovoltaic Integration," *IEEE Transactions on Sustainable Energy*, vol. 10, no. 1, pp. 280–289, 2019.

[21] A. Zhou, M. Yang, M. Wang, and Y. Zhang, "A Linear Programming Approximation of Distributionally Robust Chance-Constrained Dispatch with Wasserstein Distance," *IEEE Transactions on Power Systems*, vol. 35, no. 3, pp. 3366–3377, 2020.

[22] R. Zhu, H. Wei, and X. Bai, "Wasserstein Metric Based Distributionally Robust Approximate Framework for Unit Commitment," *IEEE Transactions on Power Systems*, vol. 34, no. 4, pp. 2991–3001, 2019.

[23] P. Mohajerin Esfahani and D. Kuhn, "Data-driven distributionally robust optimization using the Wasserstein metric: performance guarantees and tractable reformulations," *Mathematical Programming*, vol. 171, pp. 115–166, 2018.

[24] S. Huang, Q. Wu, Z. Liu, and A. H. Nielsen, "Review of Congestion Management Methods for Distribution Networks with High Penetration of Distributed Energy Resources," in *Proc. IEEE Innovative Smart Grid Technologies Europe (ISGT Europe)*, Istanbul, Turkey, 2014, pp. 1–6.

[25] S. Huang, Q. Wu, S. S. Oren, R. Li, and Z. Liu, "Distribution Locational Marginal Pricing Through Quadratic Programming for Congestion Management in Distribution Networks," *IEEE Transactions on Power Systems*, vol. 30, no. 4, pp. 2170–2178, 2015.

[26] S. Huang, Q. Wu, L. Cheng, Z. Liu, and H. Zhao, "Uncertainty Management of Dynamic Tariff Method for Congestion Management in Distribution Networks," *IEEE Transactions on Power Systems*, vol. 31, no. 6, pp. 4340–4347, 2016.

[27] S. Acharya, Y. Dvorkin, H. Pandzic, and R. Karri, "Cybersecurity of Smart Electric Vehicle Charging: A Power Grid Perspective," *IEEE Access*, vol. 8, pp. 214 434–214 453, 2020.

[28] A. Sheikh, V. Kamuni, A. Patil, S. Wagh, and N. Singh, "Cyber Attack and Fault Identification of HVAC System in Building Management

Systems," in *Proc. 9th International Conference on Power and Energy Systems (ICPES)*, Perth, Australia, 2019, pp. 1–6.

[29] M. E. Baran and F. F. Wu, "Optimal Capacitor Placement on Radial Distribution Systems," *IEEE Transactions on Power Delivery*, vol. 4, no. 1, pp. 725–734, 1989.

[30] N. Nazir and M. Almassalkhi, "Grid-aware aggregation and realtime disaggregation of distributed energy resources in radial networks," *IEEE Transactions on Power Systems*, Early Access, 2021.

[31] T. Niu, Q. Guo, H. Sun, Q. Wu, B. Zhang, and T. Ding, "Autonomous Voltage Security Regions to Prevent Cascading Trip Faults in Wind Turbine Generators," *IEEE Transactions on Sustainable Energy*, vol. 7, no. 3, pp. 1306–1316, 2016.

[32] T. Niu, H. Liu, Q. Guo, H. Lan, H. Sun, Y. Wang, B. Wang, and X. Liu, "Wind Farm Side Optimal Power Flow Based on DistFlow and SOCP: Model and Case Study," in *Proc. IEEE PES Asia-Pacific Power and Energy Engineering Conference (APPEEC)*, HongKong, 2014, pp. 1–5.

[33] J. A. Taylor and F. S. Hover, "Convex Models of Distribution System Reconfiguration," *IEEE Transactions on Power Systems*, vol. 27, no. 3, pp. 1407–1413, 2012.

[34] M. Farivar, L. Chen, and S. Low, "Equilibrium and Dynamics of Local Voltage Control in Distribution Systems," in *Proc. 52nd IEEE Conference on Decision and Control*. Florence, Italy: IEEE, 2013, pp. 4329–4334.

[35] R. Xu, C. Zhang, Y. Xu, and Z. Dong, "Rolling horizon based multi-objective robust voltage/VAR regulation with conservation voltage reduction in high PV-penetrated distribution networks," *IET Generation, Transmission and Distribution*, vol. 13, no. 9, pp. 1621–1629, 2019.

[36] M. Farivar and S. H. Low, "Branch Flow Model: Relaxations and ConvexificationPart I," *IEEE Transactions on Power Systems*, vol. 28, no. 3, pp. 2554–2564, 2013.

[37] R. D. Zimmerman, C. E. Murillo-sánchez, and R. J. Thomas, "MATPOWER: Steady-State Operations, Planning, and Analysis Tools for Power Systems Research and Education," *IEEE Transactions on Power Systems*, vol. 26, no. 1, pp. 12–19, 2011.

[38] Q. Wu, A. H. Nielsen, J. Østergaard, S. T. Cha, F. Marra, Y. Chen, and C. Træholt, "Driving Pattern Analysis for Electric Vehicle (EV) Grid Integration Study," in *Proc. IEEE PES Innovative Smart Grid Technologies Conference Europe (ISGT Europe)*, Gothenberg, Sweden, 2010, pp. 1–6.

[39] T. Hastie, R. Tibshirani, and J. Friedman, *The Elements of Statistical Learning: Data Mining, Inference, and Prediction*, 2nd ed. Springer Science & Business Media, 2009.

[40] B. Efron and R. Tibshirani, *An Introduction to the Bootstrap*. Chapman & Hall/CRC Press, 1994.

[41] Y. Cao, S. Tang, C. Li, P. Zhang, Y. Tan, Z. Zhang, and J. Li, "An Optimized EV Charging Model Considering TOU Price and SOC Curve," *IEEE Transactions on Smart Grid*, vol. 3, no. 1, pp. 388–393, 2012.

[42] S. Huang, Q. Wu, L. Cheng, and Z. Liu, "Optimal Reconfiguration-Based Dynamic Tariff for Congestion Management and Line Loss Reduction in Distribution Networks," *IEEE Transactions on Smart Grid*, vol. 7, no. 3, pp. 1295–1303, 2016.

[43] S. S. Saha, D. Arnold, A. Scaglione, E. Schweitzer, C. Roberts, S. Peisert, and N. G. Johnson, "Lyapunov stability of smart inverters using linearized distflow approximation," *IET Renewable Power Generation*, vol. 15, no. 1, pp. 114–126, 2021.